International Journal of Electrical and Electronics Engineering (IJEEE)
ISSN(P): 2278-9944; ISSN(E): 2278-9952
Vol. 5, Issue 5, Aug – Sep 2016, 25-36

International Academy of Science, Engineering and Technology
Connecting Researchers; Nurturing Innovations

EFFECTIVENESS OF SPEED SENSOR AND SENSOR-LESS CONTROLLER IN A GRID CONNECTED DFIG BASED WT SYSTEM - A COMPARATIVE STUDY

SUBIR DATTA

Department of Electrical Engineering, Mizoram University Aizawl, Mizoram, India

ABSTRACT

This paper presents the performances of a grid connected DFIG based WT system with and without speed sensor and their effectiveness have been compared. Performances of the controller have been demonstrated through time domain simulation studies. Simulation results have been compared and conclusions have been drawn. Results show that the satisfactory operation of speed sensor-less system under varying wind speed power generation as that of speed sensor controller.

KEYWORDS: Wind Energy Conversion System (WECS), Doubly Fed Induction Generator (DFIG), and Speed Sensor-Less Controller

INTRODUCTION

Now-a-days, DFIG-WT system has become one of the most popular wind generator systems. The back-to-back converter has two main parts: Grid Side Converter (GSC) to rectify grid voltage and Rotor Side Converter (RSC) to feed controllable voltage to the rotor circuit of DFIG [1]. Power electronics converter processes only the slip power. Therefore it is designed in partial scale, for just about 30% of generator rated power [2]. This causes reduction in converter cost, injection of less harmonics to the grid, improves overall energy conversion efficiency [3-6] and further, there exists scope for independent control of active and reactive powers. The DFIG can act as a variable speed generator in stand-alone and grid connected applications. In both cases, speed sensor-less vector control is desirable as shaft sensors have drawbacks in terms of maintenance, cost, robustness and cabling between the sensors and controllers and encoder failure is one of the most significant failure modes of these systems. Sensor-less vector control systems for doubly fed induction machines have been previously published by several researchers. Most are based on open loop methods, where the estimated and measured rotor currents are compared in order to derive the rotor position [7-10] and the speed then obtained via differentiation. However, for the open loop methods proposed in [7-10], the observer modeling and design methodology for the whole sensor-less system are not discussed. In [11,12], an observer based on the magnetizing current derived from the rotor and the stator equations of the machine was proposed, although on methodology was proposed for the observer modeling and design. In [13,14] rotor flux based schemes are proposed, where the rotor flux is obtained by integrating the rotor back e.m.f. The methods have poor performance at the synchronous speed due to low frequencies in the rotor so that the flux cannot be accurately estimated by integrating the rotor voltages. Model reference adaptive system observers are well known for sensor-less control of squirrel cage induction machines [15-17] and have many advantages compared to other speed estimation methods [15]. In [18] several MRAS observers are investigated: these are based on stator flux, rotor flux, rotor current and stator current as the error variable. The advantages and disadvantages of each of the MRAS observers, for stand-alone and grid connected operation, are discussed in [18]. In[19], a speed sensor less reactive power

based MRAS control scheme was proposed where information of rotor speed or position is not required for field orientation of the rotor variables. But this method cannot estimate the value of slip speed (ω_{slip}) correctly as this method is more sensitive on machine parameters and a no line magnetizing inductance (L_m) estimator is required to estimate the value of ω_{slip}. Hence, the method is quite complex and cannot estimate slip speed correctly. In [20], a modified speed sensor-less control scheme was presented which is designed with three phase rotor current based PLL. In this paper, the performances of a speed sensor [21] and sensor-less [20] based grid connected DFIG based WT system have been studied and their effectiveness have been compared. Initially, simulation model of a 2.5MW DFIG-WT system has been developed in MATLAB/Simulink environment.

BACK-TO-BACK CONVERTER-BASED DFIG-WT SYSTEM

Figure 1 shows the block diagram of the overall system (comprising of grid-connected variable speed DFIG-WT, back-to-back converter) along with the control scheme. Stator terminals of DFIG are directly connected to the grid whereas the rotor terminals are connected to the same grid, but via a PWM-based conventional back-to-back converter which comprises of Rotor Side Converter (RSC) and Grid Side Converter (GSC), connected through DC link [1]. The vector control of DFIG-WT is achieved by controlling RSC and GSC independently.

Rotor speed (ω_r) of DFIG can be controlled and set to the desired value (ω_{ref}) by controlling the direction and magnitude of active power flow (P_r) through its rotor. The desired speed (ω_{ref}) is that rotor speed at which the WT can extract the highest amount of power (P_{opt}) from the wind of certain velocity. Corresponding to any wind speed, P_{opt} value is obtained from the optimum power versus wind-speed curve and is considered as the reference or set active power. Actual value of active power extracted/converted into electrical power (P_s) is continuously calculated from the measured data, controlled by controlling P_r and is used to track the reference active power (P_{opt}). Once, set active power is reached, the desired rotor speed is automatically achieved. The reactive power set point has been calculated from the active power set point and desired power factor.

SPEED SENSOR-BASED VECTOR-CONTROL SCHEME OF ROTOR SIDE CONVERTER

For independent control of active and reactive power of rotor, stator field oriented reference frame has been used. RSC is controlled to get control over rotor d- and q-axis current components. In stator flux-oriented control, both stator and rotor quantities are transformed to a special reference frame that rotates at an angular frequency equal to the stator flux linkage space phasor, with the real axis (d-axis) of the reference frame aligned to the stator flux vector. At steady state, the reference frame speed equals the synchronous speed. RSC of DFIG is controlled in synchronously rotating dq-axis frame, with d-axis oriented along stator-flux vector position [21]. The PWM voltage source converter is current regulated with the d-axis current (i_{dr}) used to regulate the stator reactive power and q-axis current (i_{qr}) used to regulate the stator active power.

This control strategy of the DFIG based grid connected VSCF generator, described in the [21], uses a speed sensor/encoder to sense the speed of the machine for implementing the vector control strategy for RSC. However, speed sensor-less operation is a desirable feature for the vector-controlled DFIG, since speed sensors have many disadvantages like additional cost, extra cabling, reduced reliability and increased maintenance.

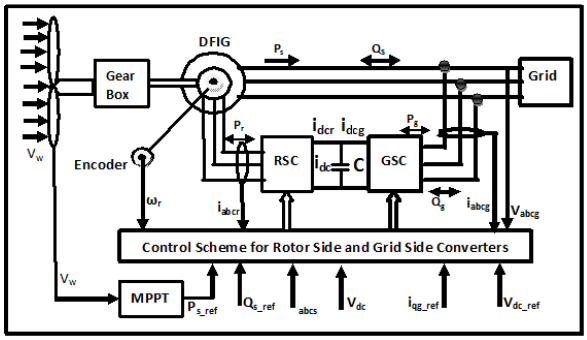

Figure 1: Grid-Connected DFIG-WT System with Control Schemes

SPEED SENSOR-LESS BASED DFIG-WECS USING BACK TO BACK CONVERTER

Similar to speed sensor-based controller, a speed sensor-less controller [20] has been developed in the stator field oriented reference frame for controlling the RSC. In this control scheme, like previous Art-III, rotor speed and position are not sensed from the generator to implement vector control strategy for RSC. Speed sensor-less controller, presented in [20], has been considered in this paper.

SIMULATION RESULTS

To compare the effectiveness of the speed sensor and sensor-less controllers based grid connected DFIG-WT system under varying wind velocity, an extensive simulation study has been carried out in MATLAB /Simulink environment on WECS system having rated wind velocity of 12m/s.

The time response of system (B2BC-based DFIG-WT) outputs have been obtained through simulation, (1) First with speed sensor-based RSC & GSC controllers, and then (2) with speed sensorless RSC & GSC controllers, to study and compare the performance of the same system. The performances have been presented: (1) in Art-A (with speed sensor) and (2) in Art-A (without speed sensor) for variation in wind speed from rated-to-below rated (8 m/s)-to-rated. The performances of the system under same wind velocity [{Art-A with Art-B}] but with two different controllers, have been compared in Art -VI.

- **Simulation results for Speed Sensor controller**

In this sub-section, steady state and transient responses of the system have been considered with speed sensor-based controller when the system is subject to wind velocity which varies from rated-to-below rated-to-rated again, as shown in Figure 2(a).

Steady State Performance: From the simulation results, it may be noted that under steady state

- When wind velocity, $V_w = V_{w,rated}$:
  - Rotor of DFIG runs at super-synchronous speed, i.e., $\omega_r > \omega_s$, [Figure 2(b)].
  - C_p attains the desired level, $C_{p,opt}$ (= 0.48) [Figure 2(c)] and remains fixed at that level indicating the performance of MPPT controller.
  - Rated active power is delivered from stator to the grid ($P_s \approx P_{rated}$) [Figure 2(d)] at $Q_s = 0$ [Figure 2(f)],
  - P_r remains –ve [Figure 2(k)] indicating that the rotor delivers active power to the grid at $i^s_{dr} = 0$, [Figure 2(i)].

- When wind velocity, $V_w < V_{w,rated}$:
  - Rotor of DFIG runs at sub-synchronous speed, i.e., $\omega_r < \omega_s$, [Figure 2(b)],
  - C_p attains the desired level, $C_{p,opt}$ (= 0.48) [Figure 2(c)] & remains fixed at that level,
  - Active power delivered from stator to the grid decreases below rated value, i.e., $P_s < P_{rated}$ [Figure 2(d)] at $Q_s = 0$ [Figure 2(f)].
  - P_r is +ve [Figure 2(k)], i.e., rotor absorbs active power from grid at $i^s_{dr} = 0$ [Figure 2(i)], i.e., at $Q_r=0$.
- The voltage across DC-link capacitor, as shown in Figure 2(m), has been found to remain fixed to its rated value irrespective to the change in wind speed. This indicates the quality of performance of the controller for GSC.
- The change in the direction of rotor power can be visualised from the waveform of rotor current also, as shown in Figure 2(k). It may be noted that the rotor current changes phase at two instants (at around 6.5 sec & 14.6 sec) of time. The phase change, at these instants, occurs due to the change of rotor speed from super-synchronous to sub-synchronous and vice-versa [shown in Figure 2(b)] causing corresponding changes in the direction of flow of rotor power, P_r as shown in Figure 2(k).
- It may be observed from the responses that all the system variables have faithfully tracked their respective reference values under the influence of the controllers and represent measure of steady state performance quality.

Transient Performance:

- Although the steady state response of MPPT controller at any of the constant wind velocities ($V_w \leq V_{wrated}$) is found to be good, a deviation has been observed in the value of C_p while tracking C_{pmax} during transient intervals (especially when subjected to ramp increase/decrease). In true sense, the transient response of MPPT controller is found to be slightly sluggish. This resulted in the deviation in tracking the speed of rotation by rotor and active power by stator [Figure 2(b)-(d)]. A major reason for the sluggish transient response of MPPT controller may be due to the presence of high inertia as rotating mechanical components of the system.
- Transient responses of C_p, ω_r & P_s during changes in wind velocity are found to be sluggish. However, transient responses of all other variables are good.

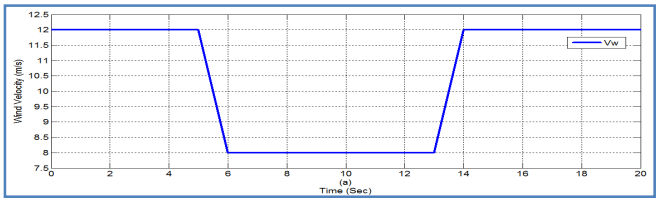

Figure 2(a): Wind Velocity (Vw)

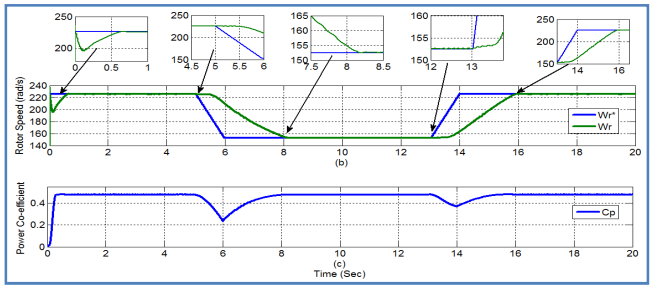

Figure 2(b): Reference and Actual Generator Speed (w_r* & w_r) and (c) C_{pmax}

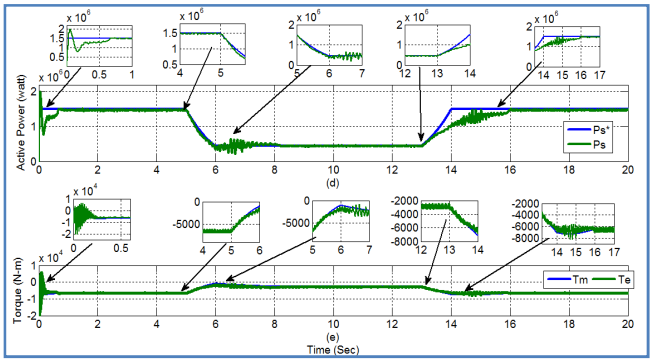

Figure 2(d): Reference & Active Power from Stator (P_s* & P_s) and (e) Mechanical & Electrical Torque (T_m & T_e)

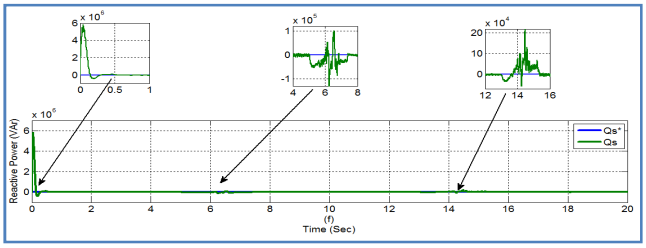

Figure 2 (f): Reference and Reactive Power from Stator (Qs*& Qs)

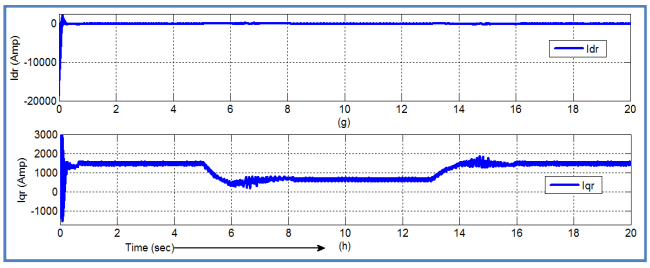

Figure 2(i): D-Axis Rotor Current (i_{dr}) and (j) q-Axis Rotor Current (i_{qr})

- **Simulation Results for Speed Sensor-Less Controller**

In this sub-Section, steady state and transient responses of the system have been presented with speed sensorless controller when the system is subject to the first set of wind velocity which varies from rated-to-below rated-to-rated again, as shown in Figure 3(a).

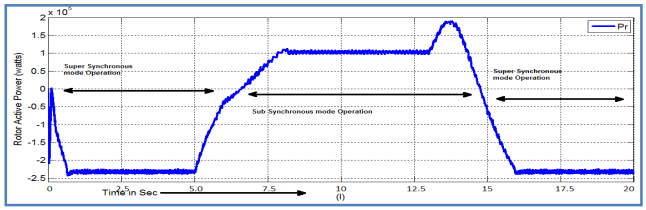

Figure 2(k): Active Power through Rotor (Pr)

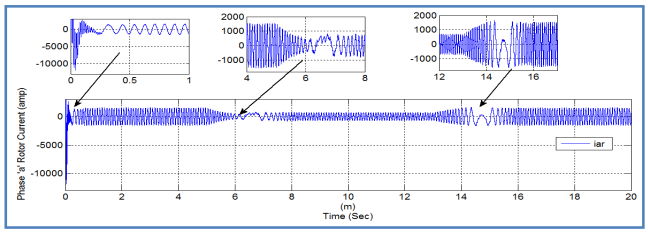

Figure 2(l): Waveform of One Phase of Rotor Current

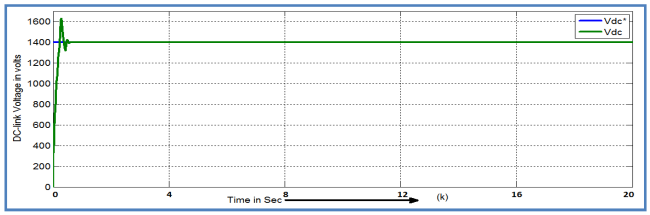

Figure 2(m): DC-Link Voltage Vdc

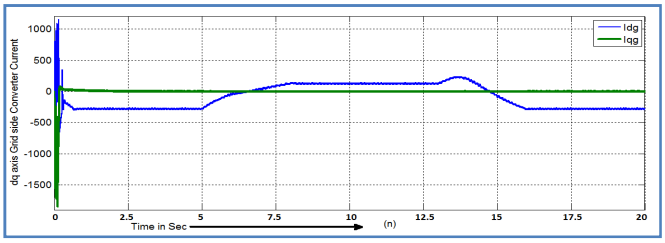

Figure 2(n): D-Axis and (o) q-Axis Currents between GSC and Grid

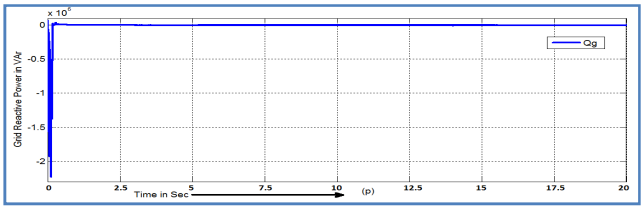

Figure 2(p): Grid Reactive Power (Q_g)

Steady State Performance: From the simulation results, it may be noted that under steady state

- When wind velocity, $V_w = V_{w,rated}$:
  - Rotor of DFIG runs at super-synchronous speed, i.e., $\omega_r > \omega_s$, [Figure 3 (b)].
  - C_p attains the desired level, $C_{p,opt}$ (= 0.48) [Figure 3 (c)] and remains fixed at that level indicating the performance of MPPT controller.
  - Rated active power is delivered from stator to the grid ($P_s \approx P_{rated}$) [Figure 3. (d)] at $Q_s = 0$ [Figure 3 (f)],

  - P_r remains –ve [Figure 3 (k)] indicating that the rotor delivers active power to the grid at $i^s_{dr} = 0$[Figure 3 (i)], i.e., at $Q_r = 0$.

- When wind velocity, $V_w < V_{w,rated}$:
  - Rotor of DFIG runs at sub-synchronous speed, i.e., $\omega_r < \omega_s$, [Figure 3 (b)],
  - C_p attains the desired level, $C_{p,opt}$ (= 0.48) [Figure 3 (c)] & remains fixed at that level,
  - Active power delivered from stator to the grid decreases below rated value, i.e., $P_s < P_{rated}$ [Figure 3 (d)] at $Q_s = 0$ [Figure 3.12(f)].
  - P_r is +ve [Figure 3.12(k)], i.e., rotor absorbs active power from grid at $i^s_{dr} = 0$ [Figure 3 (i)], i.e., at Q_r=0.
- The voltage across DC-link capacitor [Figure 3 (m)] has been found to remain fixed to its rated value irrespective to the change in wind speed. This indicates the quality of performance of the controller for GSC.
- The change in the direction of rotor power can be visualised from the waveform of rotor current also, as shown in Figure 3 (k). It may be noted that the rotor current changes phase at two instants (at around 6.5 sec & 14.6 sec) of time. The phase change, at these instants, occurs due to the change of rotor speed from super-synchronous to sub-synchronous and vice-versa [shown in Figure 3(b)] causing corresponding changes in the direction of flow of rotor power, P_r as shown in Figure 3 (k).
- It may be observed from the responses that all the system variables have faithfully tracked their respective reference values under the influence of the controllers and represent measure of steady state performance quality.

Transient Performance

- Although the steady state response of MPPT controller at any of the constant wind velocities ($V_w \leq V_{wrated}$) is found to be good, a deviation has been observed in the value of C_p while tracking C_{pmax} during transient intervals (especially when subjected to ramp increase/decrease). In true sense, the transient response of MPPT controller is found to be slightly sluggish. This resulted in the deviation in tracking the speed of rotation by rotor and active power by stator [Figure 3 (b)-(d)]. A major reason for the sluggish transient response of MPPT controller may be due to the presence of high inertia as rotating mechanical components of the system.
- Transient responses of C_p, ω_r & P_s during changes in wind velocity are found to be sluggish. However, transient responses of all other variables are good.

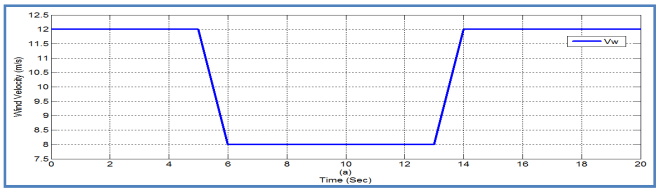

Figure 3 (a): Wind Velocity

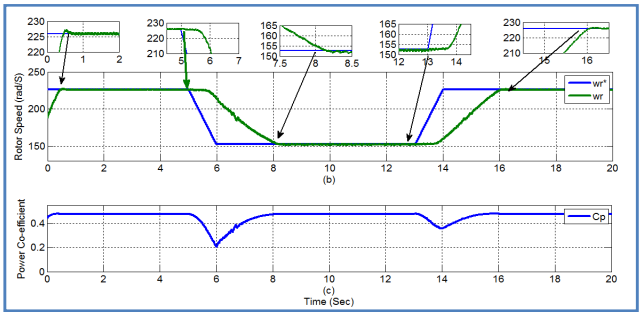

Figure 3 (b): Reference & Actual Generator Speed (w_r* & w_r) and (c) Cpmax

COMPARISON OF SYSTEM RESPONSES OBTAINED WITH AND WITHOUT SPEED SENSOR-BASED CONTROLLERS

Controller performance is decided by the time-response of the system which it controls. In the present article, time responses of the B2BC-based DFIG-WT system with speed sensor-based & speed sensorless controllers have been compared.

List of variables, figures where responses with the two types of controllers are shown and the comments on responses are presented in Table 1.

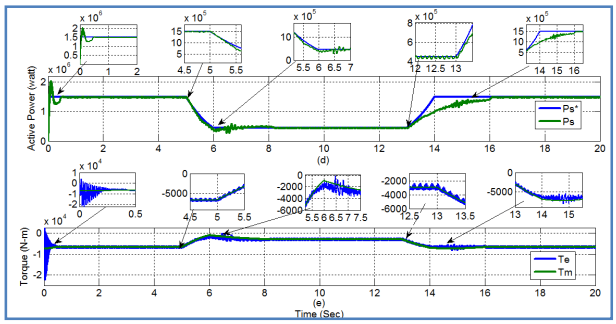

Figure 3(d): Reference & Actual Active Power (Ps*, Ps) and (e) Mechanical & Electrical Torque (Tm & Te)

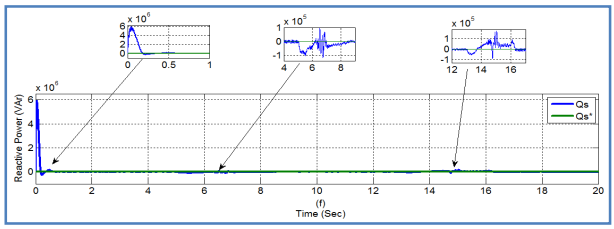

Figure 3(f): Reference & Actual Reactive Power (Qs*, Qs)

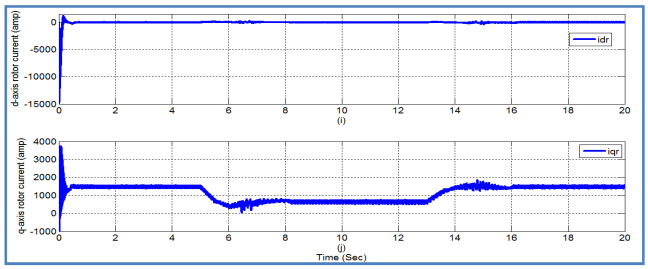

Figure 3(i): D-Axis Rotor Current (i_{dr}) & (j) q-Axis Rotor Current (i_{qr})

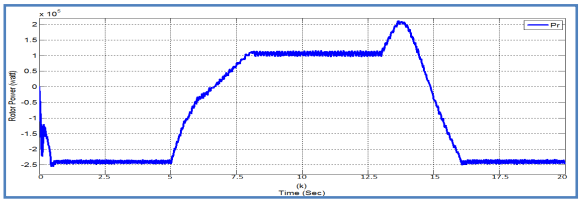

Figure 3(k): Rotor Power (Pr)

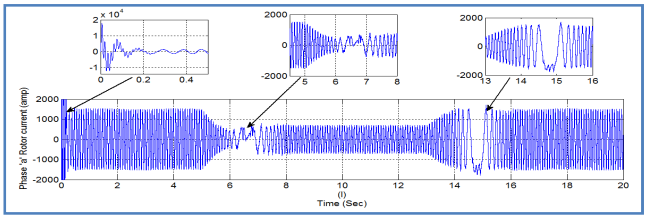

Figure 3(l): Current Waveform of One of the Phases of Rotor

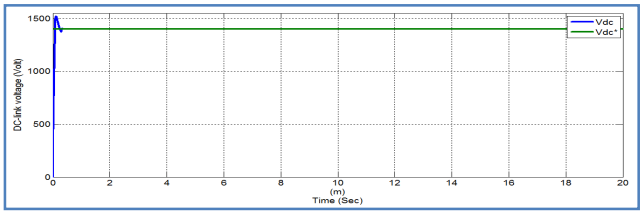

Figure 3(m): DC-Link Voltage

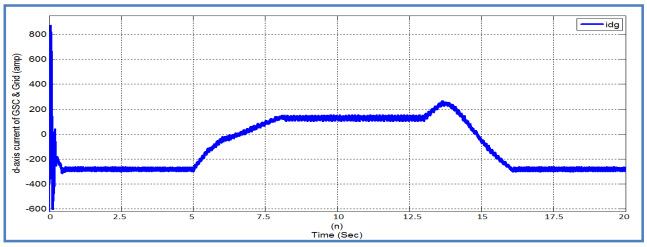

Figure 3(n): D-Axis Current of GSC & Grid

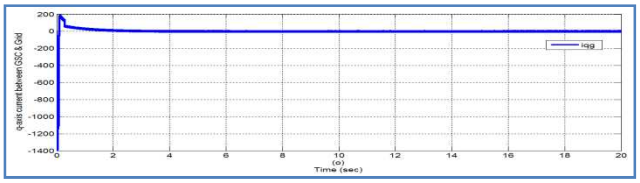

Figure 3(o): Q-Axis Current of GSC & Grid

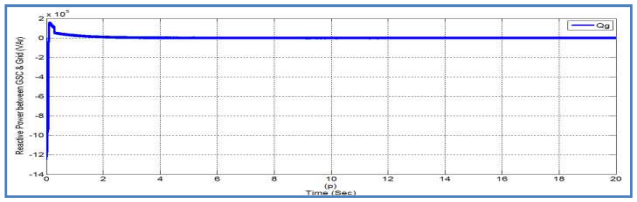

Figure 3(p): Reactive Power (Qg) between GSC & Grid

Table 1: Comparison of System Responses with Speed Sensor-Based & Sensorless Controllers

Variables	Fig No		Comments on System Response with Two Controllers when wind Velocity Varies from Rated-to-Below Rated-to-Rated Values
	With Speed Sensor	Without Speed Sensor	
Vw	2(a)	3(a)	Same type of wind velocity has been applied in both cases.
ωr	2(b)	3(b)	Steady state responses obtained with both types of controllers are equally good. Transient responses wrt rise time, settling time etc. are almost same, but few oscillations were observed to occur in the transient responses with speed sensorless controller before settlement of the variables.
Cp	2(c)	2(c)	The time response of rotor speed with and without speed sensor are almost same.
Ps	2(d)	3(d)	It may be seen that the time response of active power is same in both the cases.
Te	2(e)	3(e)	The time response of toque with and without speed sensor are almost same.
Qs	2(f)	3(f)	The time response of reactive power with and without speed sensor are almost same.
i_{dr}	2(i)	3(i)	Both the controllers have perfectly tracked the reference values of i_{dr}=0.
i_{qr}	2(j)	3(j)	Both the controllers have perfectly tracked the reference values of i_{qr}as required.
Pr	2(k)	3(k)	The time response of rotor active power with and without speed sensor are almost same.
V_{dc}	2(m)	3(m)	Both the controllers have perfectly tracked the reference DC-link voltage value.
Q_g	2(p)	3(p)	Both the controllers have perfectly tracked the reference values of Q_g=0 for unity power factor operation.

CONCLUSIONS

This paper has been compared the performance of a 1.5MW DFIG based variable speed WECS with and without speed sensor using back-to-back converter. The speed sensor-less controller can be used for vector control operation of RSC to ensure decoupled control of stator active and reactive power while maximising the power generation at unity power factor under varying wind speed.

The simulation results of speed sensor-less based DFIG-WT system also show satisfactory dynamic and transient operation under varying wind speed power generation as that of speed sensor controller. Hence, speed sensor controller can be replaced by speed sensor-less controller to overcome the drawbacks associated with speed sensor controller.

REFERENCES

1. Badrul H. Chowdhury, Srinivas Chellapilla, “Double –Fed Induction Generator Control for Variable Speed Wind Power Generation,” Elsevier Power System Research, 2006, pp: 786-800.
2. Holdsworth, L., X.G. Wu, J.B. Ekanayake and N. Jenkins, “Comparison of fixed speed and doubly-fed induction wind turbines during power system disturbances,” IEE Proc. Gener. Transm. Distrib., 150 (3): 343-352, 2003.
3. Li, G., M. Yin, M. Zhou and C. Zhao, “Decoupling control for multi terminal VSC HVDC based wind farm interconnection,” IEEE Power Engineering Society General Meeting, 2007, pp.1-6.
4. R.G. Almeida, E.D. Castronuovo, J.A. Pacas Lopes, “Optimum Control in Wind Parks when Carrying out system Operator Requests,” IEEE Transactions Power System. Vol.19, 2006, pp 1942-1950.

5. M.V.A. Nunes, H.H. Zurn, U.H. Bezerra, J.A. Pecas Lopes, R.G. Almeida, “Influence of the variable Speed wind Generators in Transient Stability Margin of the Conventional Generators Integrated in Electrical Grids,” IEEE Transactions on Energy Conversion. Vol. 21, 2006, pp257-264.
6. Y. Lei, A. Mullane, G. Lightbody, R. Yacamini, “ Modeling of the wind turbine with a Doubly fed Induction Generator for Grid Integration Studies,” IEEE Transactions on Energy Conversion, Vol.21, 2006, pp.257-264.
7. M. Abolhassani, P. Niazi, H. Toliyat, and P. Enjeti, “A sensor-less integrated doubly-fed electric alternator/active filter (IDEA) for variable speed wind energy system,” in *Proc. 38th IAS Annu. Meeting*, Oct. 2003, vol. 1, pp. 507–514.
8. R. Datta and V. T. Ranganathan, “A simple position sensor-less algorithm for rotor side field oriented control of wound rotor induction machine,” *IEEE Trans. Ind. Electron.*, vol. 48, no. 4, pp. 786–793, Aug.2001.
9. L. Morel, H. Godfroid, A. Mirzaian, and J. M. Kauffmann, “Double-fed induction machine: Converter optimization and field oriented control without position sensor,” *Proc. Inst. Elect. Eng.*, vol. 145, no. 4, pp. 360–368, Jul. 1998.
10. B. Hopfensperger, D. J. Atkinson, and R. A. Lakin, “Stator-flux oriented control of a doubly-fed induction machine without position encoder,” *Proc. Inst. Elect. Eng.*, vol. 147, no. 4, pp. 241–250, Jul. 2000.
11. O. A. Mohammed, Z. Liu, and S. Liu, “A novel sensor-less control strategy of doubly fed induction motor and its examination with the physical modelling of machines,” *IEEE Trans. Magnetics*, vol. 41, no. 3, pp. 1852–1855, May 2005.
12. O. A. Mohammed, Z. Liu, and S. Liu, “A novel sensor-less control strategy of doubly-fed induction machines,” in *Proc. IEEE Int. Conf. Elect. Mach. Drives*, May 2005, pp. 315–319.
13. L. Xu and W. Cheng, “Torque and reactive power control of a doubly-fed induction machine by position sensor-less scheme,” *IEEE Trans. Ind. Appl.*, vol. 31, no. 3, pp. 636–641, May/Jun. 1995.
14. S. Carmeli, F. C. Dezza, and R. Perini, “Double fed induction machine drive: Proposal of a speed sensor-less control based on a MRAS,” in *Proc. IEEE Int. Conf. Elect. Mach. Drives*, May 2005, pp. 404–410.
15. C. Schauder, “Adaptive speed identification for vector control of induction motors without rotational transducers,” *IEEE Trans. Ind. Appl.*, vol. 28, no. 5, pp. 1054–1061, Oct. 1992.
16. H. M. Kojabadi, L. Chang, and R. Doraiswami, “A MRAS-based adaptive pseudo reduced-order flux observer for sensorless induction motor drives,” *IEEE Trans. Power Electron.*, vol. 20, no. 4, pp. 930–938, Jul. 2005.
17. R. Cardenas, R. Pena, J. Proboste, G. Asher, and J. Clare, “MRAS observer for sensor-less control of stand-alone doubly-fed induction generators,” *IEEE Trans. Energy Conversion*, vol. 20, no. 4, pp. 710–718, Dec. 2005.
18. R. Cardenas, R. Pena, J. Clare, G. Asher and J. Proboste, “MRAS Observers for Sensor-less Control of Doubly-Fed Induction Generators,” *IEEE Trans. On Power Electronics, vol. 23, no. 3, may 2008.*
19. M. Pattnaik and D. Kastha, “Adaptive speed observer for a stand-alone Doubly Fed Induction Generator feeding nonlinear and unbalanced loads”, *IEEE Trans. on energy conversion, vol. 27, no. 4, December 2012.*

20. S. Datta, J. P. Mishra and A. K. Roy, " Modified Speed Sensor-less Grid Connected DFIG based WECS", *Indian Journal of Science and Technology, Vol.8, No.16, pp. 1-12, July 2015.*

21. S. Datta, J. P. Mishra and A. K. Roy, " Performance Analysis of a DFIG based Variable Speed Wind Energy Conversion System", *Discovery, Vol. 47, No. 216, pp.29-36, 2015.*